Structure and transport in multi-orbital Kondo systems

J. Kroha [a,1], S. Kirchner [a], G. Sellier [a], P. Wölfle [a], D. Ehm [b], F. Reinert [b], S. Hüfner [b], and C. Geibel [c]

[a] *Universität Karlsruhe, Institut für Theorie der Kondensierten Materie, P.O.Box 6980, 76128 Karlsruhe, Germany*
[b] *Universität des Saarlandes, F.R. 2 – Experimentalphysik, 66041 Saarbrücken, Germany*
[c] *Max-Planck-Institut for Chemical Physics of Solids, Nöthnitzer Str. 40, 01187 Dresden Germany*

Abstract

We consider Kondo impurity systems with multiple local orbitals, such as rare earth ions in a metallic host or multi–level quantum dots coupled to metallic leads. It is shown that the multiplet structure of the local orbitals leads to multiple Kondo peaks above the Fermi energy E_F, each one with its own Kondo temperature T_K, and to "shadow" peaks below E_F. We use a slave boson mean field (MF) theory, which recovers the strong coupling Fermi liquid fixed point, to calculate the Kondo peak positions, widths, and heights analytically at $T = 0$, and NCA calculations to fit the temperature dependence of high–resolution photoemission spectra of Ce compounds. In addition, an approximate conductance quantization for transport through multi–level quantum dots or single–atom transistors in the Kondo regime due to a generalized Friedel sum rule is demonstrated.

Key words: Kondo effect; Friedel sum rule; quantum dots; high–resolution photoemission spectroscopy.

1. Introduction

In realistic Kondo impurity systems [1] the local magnetic moment is often distributued over several local orbitals. For example, in rare earth ions, embedded in a metallic host, the local moment is carried by the seven 4f orbitals whose degeneracy is lifted by spin–orbit (SO) and crystal field (CF) splitting. Small quantum dots (Qdot) containing few electrons are in general comprised of several single-particle levels and can be seen as artificial atoms. Such systems, coupled to metallic leads, can be tuned to the Kondo regime as well, if the Coulomb blockade is large enough to fix the electron number on the Qdot to an odd number and, hence, the effective dot spin to 1/2. In rare–earth systems Kondo resonances have recently been observed by high–resolution photoemission spectroscopy [2,3], while the advances in nanotechnology have made it possible to perform direct tunneling spectroscopy of the Kondo resonance in Qdots [4–6].

In this contribution we show that each of the low–lying single–particle orbitals generates a many–particle Kondo resonance near the Fermi energy E_F, and we calculate their positions, widths and heights at temperature $T = 0$. The results of a Non–Crossing Approximation (NCA) calculation at finite T are compared to high–resolution photoemission spectra of the rare–earth Kondo system $CeSi_2$. Moreover, an approximate conductance quantization in multi–orbital Kondo Qdots is predicted originating from a generalized Friedel sum rule [7].

The systems discussed above can be described by the multi–orbital Anderson impurity Hamiltonian

$$H = H_{\rm kin} + \sum_{m\sigma} \varepsilon_{dm} d^\dagger_{m\sigma} d_{m\sigma} + \sum_{pm\sigma} [V_{mp} d^\dagger_{m\sigma} c_{p\sigma} + h.c.] + \frac{U}{2} \sum_{(m\sigma)\neq(m'\sigma')} d^\dagger_{m\sigma} d_{m\sigma}\, d^\dagger_{m'\sigma'} d_{m'\sigma'}, \qquad (1)$$

[1] Corr. Author. E-mail: kroha@tkm.physik.uni-karlsruhe.de

where $H_{\rm kin} = \sum_{p\sigma} \varepsilon_p c^\dagger_{p\sigma} c_{p\sigma}$ describes the conduction electron band, and $d^\dagger_{m\sigma}$, creates an electron with spin σ in the low–lying single–particle level $\varepsilon_{dm} < 0$, $m = 0, \ldots, M-1$, with ε_{d0} the (noninteracting) ground state. Electrons in any of the local orbitals have a Coulomb repulsion U and are coupled to the conduction band via the hybridization matrix elements V_{mp}. For later use we indroduce the effective couplings $\Gamma_{mm'} = \pi \sum_p V_{mp} V^*_{pm'} A_{p\sigma}(0)$, with $A_{p\sigma}(\omega)$ the conduction electron spectral function and $N(\omega) = \sum_p A_{p\sigma}(\omega)$ the density of states per spin. In the following we will assume the system to be in the Kondo regime, $\Gamma_{mm}/|\varepsilon_{dm}| \ll 1$, $U \to \infty$, and for the expansions leading to Eqs. (7), (11), and (13) below, $\Gamma_{mm}/(\varepsilon_{dm} - \varepsilon_{d0}) \ll 1$.

2. Spectral features

In 2nd order perturbation theory, the spin scattering amplitude of the local spin shows log divergences at the energies $(\varepsilon_{dm} - \varepsilon_{d0}) \ll |\varepsilon_{d0}|$ (*) and $-(\varepsilon_{dm} - \varepsilon_{d0})$ (**). These instabilities can be understood as due to spin fluctuations involving a transition of the local electron from the ground state ε_{d0} to an excited state ε_{dm} $(m > 0)$ (*) or vice versa (**) [3,8]. The positions of these resonances at $T = 0$ can be estimated analytically from a slave boson MF theory [9] for Eq. (1), since this approach recovers the strong coupling Fermi liquid fixed point [1] of the model.

In order to implement the effective restriction of no double occupancy of *all* orbitals, enforced by the strong Coulomb repulsion U, the local electron operator is represented in terms of pseudofermions $f_{m\sigma}$ and slave bosons b as $d^\dagger_{m\sigma} = f^\dagger_{m\sigma} b$, with the operator constraint $\hat{Q} := \sum_{m\sigma} f^\dagger_{m\sigma} f_{m\sigma} + b^\dagger b \equiv 1$. In a functional integral approach, the latter is imposed by the functional Kronecker delta

$$\Delta(Q-1) = \int_{-\pi T}^{\pi T} \frac{{\rm d}\lambda}{2\pi T}\, {\rm e}^{-i\beta\lambda(Q-1)} \; . \tag{2}$$

Introducing mean field and fluctuating parts r, a for the Bose field, $b = r + a$, $b^\dagger = r + a^\dagger$ and λ_0, $\tilde{\lambda}$ for the constraint field, $\lambda = -i\lambda_0 + \tilde{\lambda}$, Eq. (1) with Eq. (2) takes the form

$$H = H_{\rm kin} + \sum_{m\sigma} \tilde{\varepsilon}_{dm} f^\dagger_{m\sigma} f_{m\sigma} + \sum_{pm\sigma} [\tilde{V}_{mp} f^\dagger_{m\sigma} c_{p\sigma} + h.c.] + (\tilde{\varepsilon}_{d0} - \varepsilon_{d0})[r^2 + a^\dagger a - 1] + H_{\rm int} \tag{3}$$

with

$$H_{\rm int} = \sum_{pm\sigma} [V_{mp} a f^\dagger_{m\sigma} c_{p\sigma} + h.c.] + (\tilde{\varepsilon}_{d0} - \varepsilon_{d0}) r [a^\dagger + a]$$

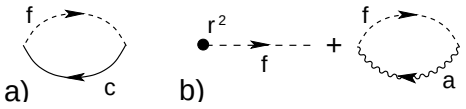

Fig. 1. Diagrammatic representation of a) the fluctuating Bose selfenergy and b) the local physical electron Green's function. The solid circle represents the modulus squared of the boson MF.

$$+ \tilde{\lambda}\Big[a^\dagger a + r^2 + r(a^\dagger + a) + \sum_{m\sigma} f^\dagger_{m\sigma} f_{m\sigma} - 1\Big] \; . \tag{4}$$

Here we have defined renormalized local levels $\tilde{\varepsilon}_{dm}$ such that $\lambda_0 = \tilde{\varepsilon}_{d0} - \varepsilon_{d0}$ and $\tilde{\varepsilon}_{dm} = \varepsilon_{dm} + \lambda_0$ and effective hybridizations $\tilde{V}_{mp} = r V_{mp}$, $\tilde{\Gamma}_{mm} = r^2 \Gamma_{mm}$. The mean field solutions r, $\tilde{\varepsilon}_{d0}$ are then obtained by minimizing the free energy, which is equivalent to setting the terms linear in the fluctuating fields a, $a^\dagger$, $\tilde{\lambda}$ equal to zero,

$$r^2 + \langle a^\dagger a \rangle + \sum_{m\sigma} \langle f^\dagger_{m\sigma} f_{m\sigma} \rangle - 1 = 0 \tag{5}$$

$$(\tilde{\varepsilon}_{d0} - \varepsilon_{d0}) r + \sum_{pm\sigma} V_{mp} \langle f^\dagger_{m\sigma} c_{p\sigma} \rangle = 0 \; . \tag{6}$$

The expectation values in Eqs. (5), (6) are calculated from the Fourier components of the pseudofermion, the mixed fermion–conduction electron, and the fluctuating boson Green's functions $G_{f\ mm'\sigma}(t) = -i\langle \hat{T} f_{m\sigma}(t) f^\dagger_{m'\sigma}(0)\rangle$, $G_{cf\ pm\sigma}(t) = -i\langle \hat{T} c_{p\sigma}(t) f^\dagger_{m\sigma}(0)\rangle$, $G_a(t) = -i\langle \hat{T} a\ (t) a^\dagger(0)\rangle$. Calculating the f selfenergies for a flat band and keeping only the leading terms in the effective hybridizations, they are [8,10],

$$G_{f\ mm\sigma}(i\omega) = \big[i\omega - \tilde{\varepsilon}_{dm} - i\tilde{\Gamma}_{mm}\big]^{-1} \tag{7}$$

$$G_{cf\ pm\sigma}(i\omega) = \tilde{V}^*_{mp}\ G_{cp\sigma}(i\omega)\ G_{f\ mm\sigma}(i\omega) \tag{8}$$

$$G_a(i\nu) = \big[i\nu - (\tilde{\varepsilon}_{d0} - \varepsilon_{d0}) - \Sigma_a(i\nu)\big]^{-1} \; . \tag{9}$$

As seen from Eq. (15) below, the low-energy peak in each of the pseudofermion spectral functions $G_{f\,mm}$ is carried over to a quasiparticle peak in the physical impurity electron spectral function, i.e. to a Kondo resonance. Hence, the width $\tilde{\Gamma}_{mm}$ of $G_{f\,mm}$ *defines* the Kondo temperature of the mth Kondo peak, $\tilde{\Gamma}_{mm} = T_{K\,m}$. It is to be determined from the MF solution below. The selfenergy of the fluctuating Bose field appearing in Eq. (5) is given by (Fig. 1 a)),

$$\mathrm{Im}\,\Sigma_a(\omega - i0) = \frac{2}{\pi} \sum_m \Gamma_{mm} \Big[\arctan\Big(\frac{\omega - \tilde{\varepsilon}_{dm}}{T_{K\,m}}\Big) + \arctan\Big(\frac{\tilde{\varepsilon}_{dm}}{T_{K\,m}}\Big)\Big] \; . \tag{10}$$

It is worth noting that Eq. (5) just represents the Friedel sum rule, when the expectation value $\langle a^\dagger a \rangle$ of the fluctuating boson density is included [8,10]. Therefore, it describes the correct shift of the Kondo resonances w.r.t. E_F due to potential scattering. We now

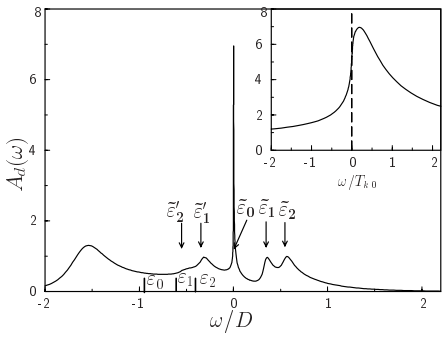

Fig. 2. local electron spectrum of the Hamiltonian Eq. (1), NCA calculation, $M = 3$. $\varepsilon_{d0,1,2} = -0.95D, -0.6D, -0.4D$, $\Gamma_{00} = \Gamma_{11} = \Gamma_{22} = 0.2D$; $T_{K0} = 3 \cdot 10^{-3}D$; $T = 5 \cdot 10^{-5}D$; D=half band width.

use the relations $\tilde{\varepsilon}_{d0} < T_{K\,0}$ and $\tilde{\varepsilon}_{dm} > T_{K\,m}$, $m = 1, \ldots, M-1$, where the former will be justified below by the MF solution in the Kondo regime, and the latter is true for sufficiently large splitting of the local levels. The positions and the widths of the Kondo peaks are then obtained from Eq. (6) and Eq. (5), respectively, as

$$\tilde{\varepsilon}_{d0} = \frac{\Gamma_{00}}{-\pi\varepsilon_{d0}}\Big(1 + \sum_{m=1}^{M-1} \frac{-2\varepsilon_{d0}\; T_{K\,m}}{\Gamma_{00}(\varepsilon_{dm} - \varepsilon_{d0})}\Big)\; T_{K\,0} \qquad (11)$$

$$\tilde{\varepsilon}_{dm} = \tilde{\varepsilon}_{d0} + (\varepsilon_{dm} - \varepsilon_{d0}) \qquad (12)$$

$$T_{K\,0} = \prod_{m=1}^{M-1} \big(\frac{D}{\varepsilon_{dm} - \varepsilon_{d0}}\big)^{\frac{\Gamma_{mm}}{\Gamma_{00}}}\; D\; \mathrm{e}^{-\frac{\pi|\varepsilon_{d0}|}{2\Gamma_{00}}} \qquad (13)$$

$$T_{K\,m} = \frac{\Gamma_{mm}}{\Gamma_{00}}\; T_{K\,0} \qquad (14)$$

Finally, we obtain the physical electron Green's function by evaluating the diagrams shown in Fig. 1b). At $T = 0$ its imaginary part reads

$$\begin{aligned} A_{d\sigma}\,(\omega) \simeq & \sum_m \frac{T_{K\,m}}{\Gamma_{mm}} \mathrm{Im} G_{f\,mm\sigma}(\omega - i0) \\ & - \Big[\Theta(\tilde{\varepsilon}_{d0} - \omega) - \frac{1}{2}\Big]\; \mathrm{Im}\Big[-\omega + \tilde{\varepsilon}_{d0} + \varepsilon_{d0} \\ & - \sum_m \frac{\Gamma_{mm}}{\pi} \ln \frac{(\omega + \tilde{\varepsilon}_{dm} - \tilde{\varepsilon}_{d0})^2 + T_{K\,m}^2}{\tilde{\varepsilon}_{dm}^2 + T_{K\,m}^2} \\ & - i\mathrm{Im}\Sigma_a(\omega - i0) - i\;\mathrm{sgn}\omega\; T_{K\,0}\Big]^{-1} . \end{aligned} \qquad (15)$$

It is seen that the first line of Eq. (15) represents multiple Kondo resonances above E_F with the positions, widths, and heights given by Eqs. (11)–(14). The remainder of Eq. (15) describes the structure below E_F. The single–particle resonance (ε_{d0}) is strongly renormalized downward due to the logarithmic terms. The maxima of the log terms indicate weak peaks or often merely shoulders at energies

$$\tilde{\varepsilon}'_{dm} = -(\tilde{\varepsilon}_{dm} - \tilde{\varepsilon}_{d0})\;, \qquad (16)$$

i.e. at mirrorimaged positions w.r.t. $\tilde{\varepsilon}_{d0}$. In contrast to the resonances above E_F, these mirrored peaks do not correspond to quasiparticle resonances, since there is no pole in $A_{d\sigma}$ at these energies. Physically, they originate from spin fluctuations involving a virtual transition from an excited state ($m \geq 1$) to the ground state ($m = 0$). This is only a virtual process, as the $m \geq 1$ states are not thermally occupied at $T = 0$ [8]. With increasing T, $0 < T < T_{K\,m}$, the peaks below E_F grow, as the $m \geq 1$ states become thermally occupied. The multiple peak structure discussed above is shown in Fig. 2. Fig. 3 shows fits of the NCA calculation of A_d to photoemission spectra of the Kondo system $CeSi_2$ ($M = 7$) [11]. The experimental data show the appearance of low–energy peaks above E_F at elevated T, in quantitative agreement with the T dependence expected theoretically from multiple Kondo resonances.

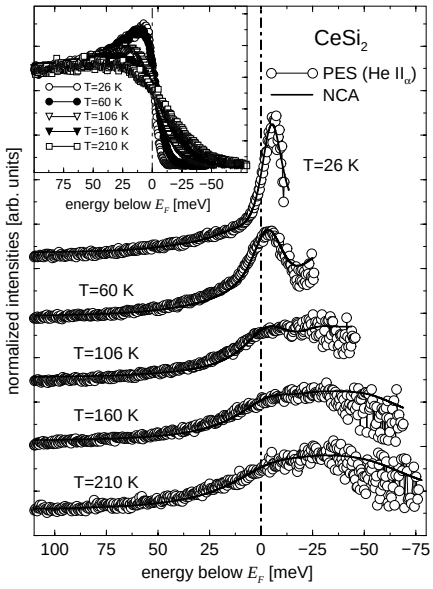

Fig. 3. Low-energy high resolution photoemission spectra of $CeSi_2$. Open circles: Experiment; solid lines: NCA. Model parameters determined from fits to the theory: ε_{d0}=-1.35 eV, SO splitting: 270 meV, CF splitting: 25 meV (lower quartet), 48 meV (upper sextet); $D = 3.7$ eV; $T_{K0} \approx 35$ K. The inset shows raw data before division by the Fermi-Dirac distribution [3].

3. Approximate conductance quantization

We now show that in a symmetrical multi–level Qdot or a single–atom transistor (SAT) [12] at low T the linear response conductance $G = \mathrm{d}I/\mathrm{dV}(V = 0)$ is *approximately* quantized at $2e^2/h$ [7], if the Qdot or SAT is in the Kondo regime, even though there may be

several transmission channels, $m = 0, \ldots, M-1$, and the lead–to–dot coupling matrix elements V_{mp} are random. Such systems are described by the Hamiltonian Eq. (1), where, in addition, the conduction electron operators carry an index $\alpha = L, R$ indicating the left or right lead, and, hence the kinetic energy term reads, $H_{\rm kin} = \sum_{p\sigma\alpha}[\varepsilon_p - \mu_\alpha] c^\dagger_{p\sigma\alpha} c_{p\sigma\alpha}$, with $\mu_{L/R} = 0, V$ the chemical potentials in the left/right lead.

The current through a left/right symmetrical device is [13]

$$I = \frac{e}{h} \sum_\sigma \int d\omega \Big[f(\omega) - f(\omega + \frac{eV}{\hbar}) \Big] {\rm Im\,tr}\,[\Gamma G_{d\sigma}(\omega)], \tag{17}$$

where $G_{d\sigma}$ is the advanced local-orbital Green's function and Γ the lead–dot couplings $\Gamma^L_{mm'} + \Gamma^R_{mm'}$. $G_{d\sigma}$ and Γ are matrices in the space of local orbitals,

$$\left[G_d^{-1}\right]_{mm\sigma}(\omega) = \omega - \varepsilon_{d,1} - i\Gamma_{mm} - \Sigma_{mm}(\omega) \tag{18}$$

$$\left[G_d^{-1}\right]_{mm'\sigma}(\omega) = -i\Gamma_{mm'} \qquad m \neq m' \ , \tag{19}$$

where $\Sigma_{mm}(\omega)$ is the selfenergy due to intra–dot interactions. Since the ground state is a spin singlet [1], the quantum dot is at $T \ll T_K \equiv \min[T_{K\,m}]$ a pure potential scatterer for electrons traversing the system, and the following Fermi liquid relations hold [14],

$$\Sigma''_m(\omega) = \frac{(\hbar\omega)^2 + (\pi k_B T)^2}{k_B T_K} \qquad \omega, T < T_K \tag{20}$$

$$\int_{-\infty}^{0} d\omega \ {\rm tr}\Big\{ \frac{\partial \Sigma(\omega)}{\partial \omega} \cdot G_{d\sigma}(\omega) \Big\} = 0 \tag{21}$$

The averaged electron number in the dot per spin, $n_{d,\sigma}$, can now be evaluated using the general relation $\frac{d}{d\omega} \ln({G_d}^{-1}) = (1 - \frac{d\Sigma}{d\omega}) \cdot G_d$ and the Luttinger theorem Eq. (21),

$$n_{d\sigma} = {\rm Im} \int_{-\infty}^{0} \frac{d\omega}{\pi} {\rm tr}\ G_{d\sigma}(\omega) = \frac{\rm Im}{\pi} \Big[{\rm tr}\{\ln\, G_{d\sigma}(\omega)^{-1}\} \Big]_{-\infty}^{0}$$

This is a statement of the Friedel sum rule $n_{d\sigma} = \frac{1}{\pi} \sum_m \delta_{m\sigma}(0)$, since the scattering phase shift at the Fermi level in channel m is $\delta_{m\sigma}(0) = \arg[\Gamma \cdot G_{d\sigma}(0)]_{mm}$. It may be re-expressed, using ${\rm tr\ ln}\ {G_{d\sigma}}^{-1} = \ln \det {G_{d\sigma}}^{-1}$, as

$$n_{d\sigma} = \frac{1}{\pi} {\rm arccot} \left[\frac{{\rm Re\ det}\ G_{d\sigma}(0)^{-1}}{{\rm Im\ det}\ G_{d\sigma}(0)^{-1}} \right] . \tag{22}$$

The scattering T-matrix of the device, $\Gamma \cdot G_{d\sigma}$, which determines the conductance $G = dI/dV$ of the system via Eq. (17), is now evaluated by expressing the inverse matrix Eqs. (18), (19) in terms of its determinant, and, using the Fermi liquid property Eq. (20), we obtain at the Fermi energy ($\omega = 0$, $T \ll T_K$) for $M = 2$,

$$\begin{aligned} &{\rm Im\ tr}\ (\Gamma \cdot G_\sigma(0)) = \sin^2(\pi n_{d\sigma}) \\ &+ \sin(2\pi n_{d\sigma}) \frac{\Gamma_{21}\Gamma_{12} - \Gamma_{11}\Gamma_{22}}{\Gamma_{11}(\varepsilon_{d,2} + \Sigma'_2(0)) + \Gamma_{22}(\varepsilon_{d,1} + \Sigma'_1(0))} \ . \end{aligned} \tag{23}$$

If the transition amplitudes V_{mp} are independent of the lead channels p, it follows directly from the definition of $\Gamma_{mm'}$ that the term $\propto \sin(2\pi n_{d\sigma})$ cancels. Eq. (23) is an exact result, valid for arbitrary microscopic parameters $\Gamma_{mm'}$, ε_{dm}, U, and $n_{d\sigma}$. It is the generalization of the well-known unitarity rule of the single-level Anderson impurity problem to the case of several impurity levels [7]. If there is at least one of the local levels significantly below the Fermi level ($\varepsilon_{d0} < 0$, $|\varepsilon_{d0}|/\Gamma_{mm'} < 1$), a strong Coulomb repulsion U enforces $n_{d\sigma} \approx 1/2$, implying via Eqs. (23), (17) a conductance close to the conductance unit, i.e. $dI/dV \approx 2e^2/h$ (the factor 2 reflects spin summation).

Acknowledgements

Stimulating discussions with C. Cuevas, A. Rosch, and E. Scheer are gratefully acknowledged. This work was supported by CFN and SFB195 of the Deutsche Forschungsgemeinschaft.

References

[1] For a comprehensive introduction see A. C. Hewson, *The Kondo Problem to Heavy Fermions* (Cambridge University Press, 1993), and references therein.

[2] Garnier *et al.*, Phys. Rev. Lett. **78** (1997) 4127.

[3] F. Reinert *et al.* Phys. Rev. Lett. **87** (2001) 106401.

[4] S. M. Cronenwett, T. H. Oosterkamp, and L. P. Kouwenhoven, Science **281** (1998) 540.

[5] D. Goldhaber-Gordon *et al.*, Nature **391** (1998) 156.

[6] S. De Franceschi *et al.*, cond-mat/0203146 (2002).

[7] S. Kirchner, J. Kroha, and E. Scheer, NATO Science Series II, vol. **50** (Kluwer, 2001), 53.

[8] D. Ehm *et al.*, in preparation.

[9] P. Coleman, Phys. Rev. B **29** (1984) 3035.

[10] S. Kirchner, PhD thesis, Univ. Karlsruhe (2002).

[11] For details of the experimental technique see Ref. [3]; and Greber *et al.*, Phys. Rev. Lett. **79** (1997) 4465.

[12] J. Park et al., Nature **417** (2002) 722.

[13] Y. Meir and N. S. Wingreen, Phys. Rev. Lett. **68**, 2512 (1992).

[14] J. M. Luttinger, Phys. Rev. **119**, 1153 (1960); **121**, 942 (1961).